VERSIONE POST-PRINT INVIATA ALLA RIVISTA DOPO LE MODIFICHE

RICHIESTE DAI REVISORI, E CORRISPONDENTE ALLA VERSIONE PUBBLICATA

REVERSE MICELLES ENHANCE THE FORMATION OF CLATHRATE HYDRATES OF HYDROGEN

Pietro Di Profio,[a,b*] Valentino Canale,[a] Raimondo Germani,[b] Simone Arca,[c] Antonella Fontana[a]

[a] Department of Pharmacy, University of Chieti-Pescara "G. D'Annunzio", Via dei Vestini 31 - I-66013 Chieti, Italy

[b] Center of Excellence on Innovative Nanostructured Materials (CEMIN), Department of Chemistry, Biology and Biotechnology, University of Perugia Via Elce di Sotto 8, I-06123 Perugia, Italy

[c] RDPower s.r.l., str. delle Campore 11/13, 05100 Terni, Italy

*Corresponding author. *E-mail address*: pietro.diprofio@unich.it; tel.: +39-0871-355 4791

ABSTRACT

Hypothesis: Clathrate hydrates of hydrogen form at relatively low pressures (e.g., ca. 10 MPa) when a co-former compound is added. In that case, however, the gravimetric amount of stored hydrogen drops to less than 1 wt% from ca. 5.6 wt% without a co-former. Another factor hindering the entrapment of hydrogen into a clathrate matrix appears to be of a kinetic origin, in that the mass transfer of hydrogen into clathrates is limited by the macroscopic scale of the gas-water interfaces involved in their formation. Thus, the enhanced formation of binary (hydrogen + co-former) hydrates would represent a major achievement in the attempt to exploit those materials as a convenient means for storing hydrogen.

Experiments: Here, we present a simple process for the enhanced formation of binary hydrates of hydrogen and several co-formers, which is based on the use of reverse

micelles for reducing the size of hydrate-forming gas-water interfaces down to tens of nanometers. This reduction of particle size allowed us to reduce the kinetic hindrance to hydrate formation.

Findings: The present process was able to (i) enhance the kinetics of the formation process; and (ii) assist clathrate formation when using water-insoluble coformers (e.g., cyclopentane, tetrahydrothiophene).

Keywords: hydrogen hydrates, kinetics, reverse micelles, clathrates, co-formers, surfactants.

Abbreviations: CP, cyclopentane; DXL, dioxolane; DHF, 2,5-dihydrofuran; NG, natural gas, THF, tetrahydrofuran; THP, tetrahydropyran; THT, tetrahydrothiophene; W_0, water/surfactant molar ratio; AOT, dioctyl sulfosuccinate sodium salt; Nml, normal-milliliter (under Normal Conditions).

1. Introduction

Hydrogen storage is one of the major issues hindering the development of the so-called *hydrogen economy*. To date, the main approaches for storing hydrogen are: 1) pressurization up to 70 MPa, 2) liquefaction at 20K, 3) adsorption onto metal hydrides, and 4) complexation to other inorganic and organic compounds, which methods all have drawbacks.[1-4] Storing hydrogen as a pressurized gas requires heavy-duty containers, and the pressures required to obtain an economically viable mass ratio are inherently hazardous,[5] and the cost of composite materials for high-pressure containers is high.[6] Storing hydrogen as a liquid also poses safety and technological problems; further, a large fraction of the stored energy is lost when converting hydrogen gas to the liquid phase, and keeping it as a liquid under extreme temperatures (22K). On the other hand, inorganic

and organic supports (metals, intermetallic compounds, carbon nanotubes, etc.) can adsorb reversibly variable amounts of hydrogen at ambient temperature and pressure; however, desorption therefrom requires a high energy input and usually takes place at elevated temperatures.[4,7]

Clathrate hydrates are ice-like compounds that form under low temperatures and high pressures. In hydrates, water molecules enclose small guests such as methane, carbon dioxide, tetrahydrofuran, hydrogen, etc., into a hydrogen-bonded, crystal network of Eulerian polyhedra.[8] Hydrates are studied, *inter alia*, because their plug oil and gas pipelines,[9,10] and are being exploited as a potential means for gas mixture separation,[11] and gas storage and transportation.[12-14] Main crystal structures for hydrates were determined by crystallographic methods, as structure I (sI), structure II (sII) and structure H (sH). A comprehensive review of crystallographic methods and hydrate structures is reported in the reference book by Sloan and Koh.[8]

Since 1999, it has been known that hydrogen forms clathrate hydrates under very high pressure/low temperature.[15,16] In 2002, Mao et al. found that hydrogen hydrate crystallizes in structures labeled as structure-II (sII) clathrates.[17,18] The structure of the hydrogen clathrate was resolved by neutron diffraction as a function of pressure and temperature. The hydrogen occupancy in the clathrate was found to change proportionally to changes in pressure and/or temperature, while leaving the host structure virtually intact. Use of a co-former (e.g., THF) drastically reduces the equilibrium pressure of hydrogen hydrates,[19] thus potentially opening the way to a clathrate hydrate-based technology for hydrogen storage.[20-22] THF turns out to be particularly suitable as a co-former, mainly due to its complete miscibility with water, while less water-soluble co-formers present inherent experimental difficulties due to the poor mass transfer in the water phase.[23]

Strobel, Sloan et al.[24, 25] and Peters and Sloan[26] recognized the need of increasing the gas-water exchange surface to increase hydrogen uptake. Notably, this was accomplished by using, *inter*

alia, milled ice particles which were sieved down to ca. 50 μm in size. However, the milled ice/THF hydrate method of, e.g., Strobel et al. required previous formation of a solid THF hydrate at 250K, then this solid hydrate was subjected to H_2 pressure to form the binary hydrate. Moreover, in some of Strobel's works,[24] either long times (several hours to days) or higher pressures (15 to 40 MPa) were employed. Loskhin and Zhao[27] also described a method for hydrogen clathrate hydrate synthesis, in which ice and hydrogen gas are firstly supplied to a container at a first temperature and pressure, and then the container is pressurized with hydrogen gas to a second, higher pressure, where hydrogen clathrate hydrates are formed in the process. In those references, besides the inherent difficulties of enclosing hydrogen into clathrate cages, due to the small size and high fugacity of H_2 molecules, also the problem of an efficient mass transfer between the gaseous and the liquid and/or hydrate phases is acknowledged and discussed.

On the other hand, Irvin et al.[28] recognized that reverse micelles can be used to increase the surface area of gas-water contact in the formation of methane and carbon dioxide hydrates. However, the authors did not suggest the use of reverse micelles for enhancing hydrogen hydrate formation, nor they recognized the role of the bulk organic solvent in the solubilization of poorly water-miscible molecules, e.g. a water-insoluble co-former. Methods are also known for the extraction of organic molecules from W/O microemulsions under hydrate forming conditions,[29] and several papers were recently published on the combined use of W/O microemulsions and hydrates for the separation of gas mixtures,[30-32] as a means for thermal energy storage,[33] and W/O microemulsions in the form of ice slurries in crude oil as a model for NG hydrates for viscosity and yield stress studies.[34] Lee et al.[35] discussed the feasibility of obtaining high-content binary hydrates of THF and hydrogen, but their process takes weeks to complete.

In the present paper, we present a kinetically efficient method for preparing hydrogen hydrates, which is based on the formation of amphiphile-aided reverse micelles. The obtained micelles were

macroscopically homogeneous, and the resulting water droplets could then be induced to form hydrate nanoparticles when the system was put under the appropriate P and T conditions. According to this method, binary co-former/hydrogen hydrates up to 0.5 wt% H_2 were obtained, with formation kinetics in the range of minutes. While this figure may seem quite low as compared to the current targets for hydrogen storage of 4.5 wt% (see, e.g., the U.S. Department of Energy website), it should be considered that hydrogen hydrates have the highest usable, specific energy content among known storage materials. Specifically, a 0.5 wt% H_2 in hydrate form corresponds to a usable energy content which is slightly higher than that provided by the same weight of H_2 pressurized at 200 bar.[36]

The present method also allows for a broader choice of water-insoluble co-formers, with the bulk organic phase serving as a reservoir of the co-former which is kept ready for hydrate formation. On the other hand, the bulk dispersing phase may also act as a "partition buffer" with the aim of limiting the concentration of very water-soluble co-formers (e.g., THF) into the water droplets, thus potentially allowing to enhance the concentration of the hydrate former (e.g., H_2) in water. Furthermore, the reaction system can be kept under homogeneous conditions, thus avoiding clogging of the reactor due to agglomeration of hydrate particles. Indeed, hydrate nanocrystals which form from the water pools precipitate to the bottom of the reactor in form of a slurry which is free-flowing; this may be advantageous in case of a scale-up to a continuous production plant. The present process can be made continuous by simply replenishing water and co-former to the shrinking water pools, thus ideally leading to a continuous production of hydrogen hydrate.

2. Materials and Methods

2.1 Materials

The structural and functional characteristics of a reverse micelle are extremely variable, and strongly dependent on the amphiphilic molecules used to stabilize their interfaces. A limited number of reverse micelle-forming molecules are known in the art, most of which refer to particular classes of anionics (AOT, the Tweens, the Spans) or non ionics (Shell's NEODOLs) amphiphiles.[30,31] We used a well known reverse micelle stabilizer (AOT from Sigma-Aldrich), with iso-octane (Sigma-Aldrich, anhydrous 99.8%) as a bulk organic phase. H_2 was Alphagaz 1, (Air Liquide); ultra-pure water (0.05 μS) was from a Millipore model Elix 3 ion-exchanger.

In a typical reverse micelle preparation to be subjected to hydrogen hydrate formation, 200 ml of iso-octane as a dispersing medium are used, and a proper amount of AOT is dissolved in the solvent, so as to obtain a concentration of 0.1M AOT in iso-octane. Then water is added in such an amount to keep the system within the stability region of the reverse micelle and avoiding phase separation (typically, 32 mL at $W_0 = 80$). Finally, a co-former is added in an amount depending of its partition equilibrium between water and the organic solvent, and also depending on the target amount of co-former in the final hydrate structure. In the experiments presented herein, co-formers were added at around their "stoichiometric" ratio to water, i.e. 5.6 mol%. Hydrate formation experiments were performed at least in triplicate, with coefficients of variation for H_2 occupancy and formation times always less than 15% (see below). Variabilities of induction times were much higher, and in the range of a few minutes to a few hours.

2.2 Apparatus

Hydrate formation was carried out into a fully controlled, AISI 316L stainless steel reactor, which has been designed and assembled by RDPower srl (Terni, Italy), having an internal volume of 500 mL, with operating pressures reaching up to 20 MPa. The reactor was equipped with cooling/heating Peltier units which allowed operating temperature ranges from 253 K to 353 K. A

chiller with a cooling power of 1000 W was used as heat sink for the Peltier units. The contents were stirred with a magnetic-coupled stirring rod to 100 rpm. While loading the reactor, the gas flow was regulated by means of a CC Series micro-metering valve (Tescom, USA). The gas flow was measured by a F131M series thermal mass flow meter (Bronkhorst High-Tech B.V., The Netherlands) with a measuring range of 5-500 NmL/min and operating pressure of 40 MPa. Gas replenishment into the reactor during hydrate formation was done by a combination of a Kammer electro-pneumatic actuator and low-flow globe valve, both from Flowserve (USA). The reactor was provided with a 4-20 mA pressure transducer (Gems Sensors & Controls, UK) with a measuring range of 0-25 MPa. Two further pressure transducers were assembled along the gas loading line before and after the metering valve in order to measure the pressure during the mixture preparation process. Resistive temperature detectors (RTD) PT100 class 1/3 DIN (OMEGA Engineering, INC., USA) were also installed. A homemade process controller for pressure, temperature, and gas flow was assembled by using an Arduino microcontroller (arduino.cc). This controller read the temperatures of each reactor and drove the Peltier power supply in order to apply cooling or heating power when required. Temperature setpoint was maintained by using a PID algorithm embedded into the Arduino controller. A schematics of the experimental apparatus is shown in Figure 1.

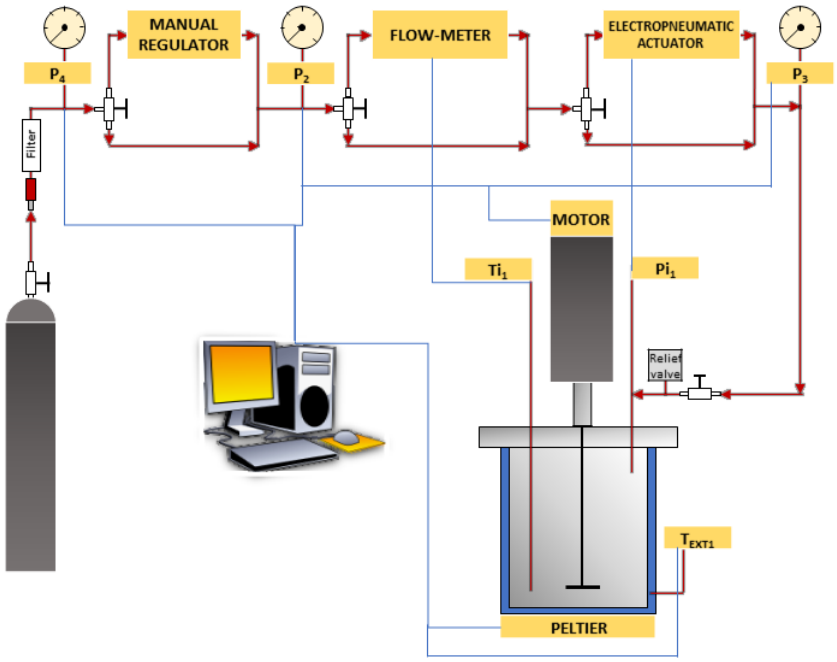

Figure 1 - Schematics of the experimental apparatus.

2.3 Dynamic Light Scattering

Dynamic light scattering (DLS) measurements were made by using ca. 1 mL of sample in 6 mm diameter Pyrex glass culture tubes, fitted into the center of a toluene-filled fluorimeter cuvette to provide refractive index matching against stray light reflections. The cuvette was housed into an aluminum cell block, whose temperature was regulated by a Peltier element. The light source was a Coherent Innova 70-3 argon-ion laser operating at 4880 Å. Light scattered at 90° was collected from approximately one coherence area and imaged onto a photomultiplier tube. A 64-channel Nicomp Model 370 computing autocorrelator (PSS Nicomp, Santa Barbara, CA) was used to calculate and display the diffusion coefficient, D, and associated derived parameters from cumulants analysis fits to the intensity autocorrelation function.[37] In particular, the second cumulant is a measure of the width of the distribution, and is related to the coefficient of variation (c_v) of the measured D value. Coefficients of variations below 10-15% are considered as a robust index of monodispersity; on the other hand, specifying individual values of c_v in the range of $0 < c_v$

< 15% is questionable. More complex relations of hydrodynamic radii with head group sizes and polydispersity (e.g., improved cumulants, Shultz distribution[38]) were not tested, as they were beyond the scope of DLS measurements in this work.

The hydrodynamic radii, R_h, could be estimated by applying the Stokes-Einstein relationship:[39]

$$D = kT/6\pi\eta R_h \qquad (1)$$

where η is the viscosity of the solution, which could be approximated to that of the dispersion phase (i.e., iso-octane).

3. Results

A typical THF-H_2 hydrate formation in a water-AOT-iso-octane reverse micelle is shown in Fig. 2, below.

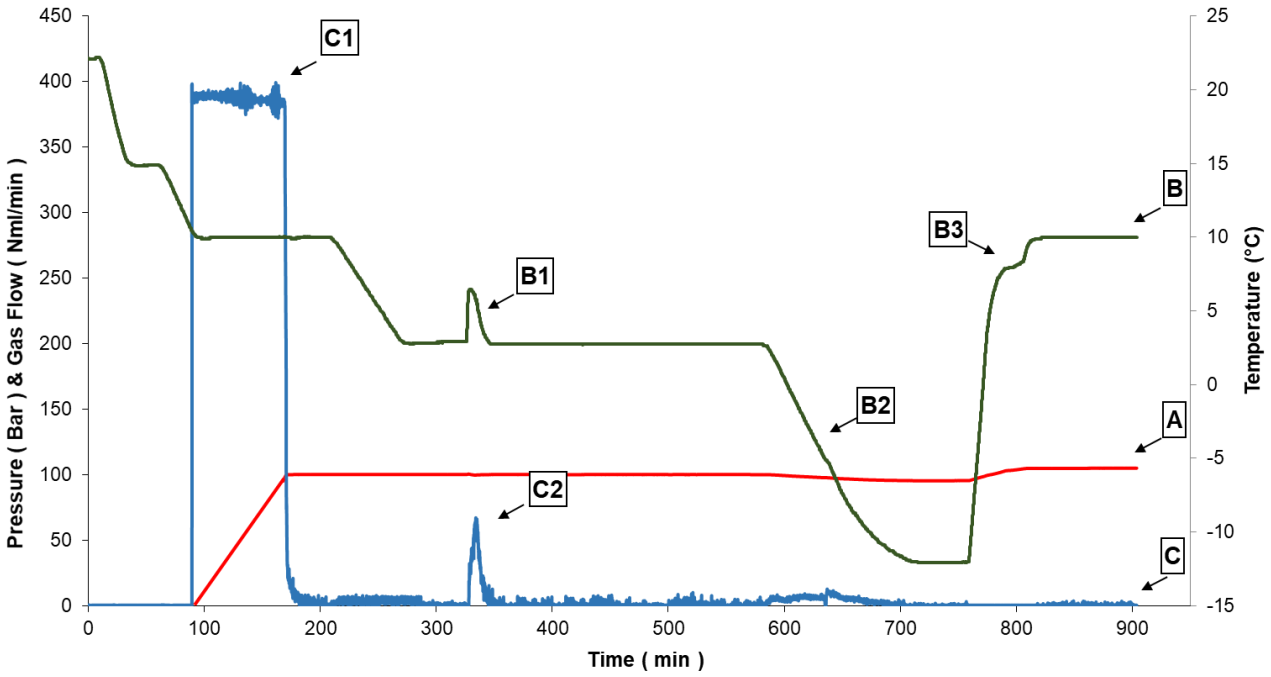

Figure 2 - P/T/Gas Flow profiles vs. time for a typical THF/H_2 hydrate formation into a reverse micelle. A: pressure; B: temperature (B1: exotherm of hydrate formation; B2: optional sub-cooling phase; B3: endotherm of hydrate dissociation); C: gas flow (C1: charging of reactor; C2: flow of hydrogen during hydrate formation).

In Figure 2, the temperature, pressure and gas flow profiles for reverse micelle-aided hydrogen hydrate formation are shown. Curve A shows the system pressure profile, where a first loading ramp is carried out up to a selected experimental pressure, and then the reactor is kept under constant pressure mode by the experimental device.[40] Curve B relates to temperature, and shows a first phase of cooling down to the formation temperature, where, after a certain induction time a peak of temperature (B1) related to the heat of formation is apparent. After all parameters were stabilized at the target set-points, an optional sub-cooling phase (B2) starts to bring the system down to a temperature below the water freezing point, -12°C in this specific case (this optional

step is carried out if the hydrate is to be recovered). After further stabilization of parameters, a warming ramp starts in order to dissociate the synthesized hydrate, for detecting the dissociation temperature indicated in B3. Curve C shows the gas flow profile, with the first constant flow step (C1) corresponding to the pressure loading phase and an absorption peak related to the hydrogen trapping in the hydrate phase (C2). The same experimental run was carried out with each co-former tested, and experimental conditions and formation temperatures are reported in Table 1 below.

Table 1: Co-formers and respective formation temperatures

Co-former	**Literature Equilibrium Temperature (K)[a,b]**	**Experimental temperature (K)[a,c]**
THF	281.2	276.2
THP	277.3	272.3
DXL	274.2	269.2
THT	279.5	274.5
CP	283.4	278.4
DHF	276.5	271.5

[a] Under 10 MPa H_2; [b] From ref. 20; [c] Effective formation temperatures investigated in the present work (see also Fig. 4).

A few words should be spent on the kinds of water which are present inside a water pool. In fact, it is known that water molecules tend to organize in at least two distinguishable regions inside a reverse micelles, i.e., a head-group hydration shell and a bulk-like region in the center.[41] Therefore, we tried to determine how much of this confined water actually forms hydrates. Figure

3 shows the results of dynamic light scattering measurements carried out on three samples of AOT reverse micelles, which differ in the amount of water and THF added; specifically, water was added in order to obtain a value of W_0 (molar ratio of water to surfactant) of 25, 50, and 80 and, for each sample, a corresponding amount of THF was added such as to keep a stoichiometric molar ratio of THF hydrate (ca. 1/17 THF/H_2O). The diameters of the reverse micelles were 13, 24 and 40 nm, respectively for the samples at W_0 = 25, 50, 80.

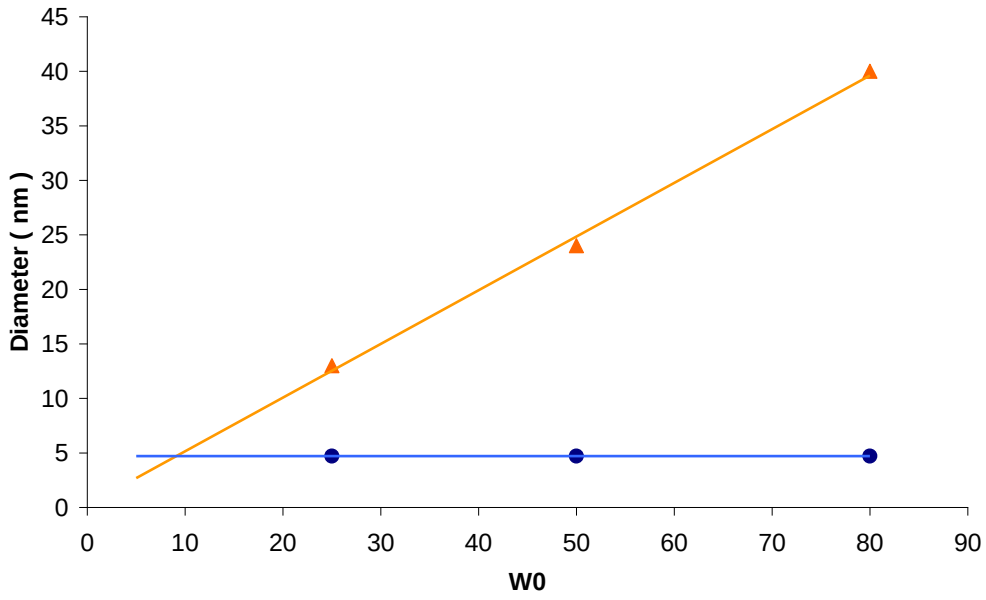

Figure 3 - Diameters of AOT-iso-octane-water-THF reverse micelles by DLS at 20°C. Triangles show the increase of micellar size as W_0 increases, while circles show the constant size of "residual" reverse micelles after hydrate formation.

Then, the samples were subjected to hydrate formation. Given the inherent difficulty of collecting DLS data inside a pressurized reactor, we used as a model a hydrate formed by co-former + water without hydrogen, which could be done under ambient pressure and at temperatures below the water-coformer hydrate equilibrium temperature (i.e. around 1°C) within standard lab glassware.

After hydrate formation, an aliquot of the remaining liquid phase was easily separated from the solid hydrate mass, returned to room temperature and again subjected to dynamic light scattering measurement. The aim of DLS measurements in this work was just to i) ensure that formed colloids were actually nano-sized; and ii) get an estimate of a residual water amount bound to the surfactant after hydrate formation. Data show a *constant size of the residual reverse micelles*, around a value of 4.4-5.0 nm (cf. Table 2, below). A linear relationship between W_0 and micelle size (D_h = hydrodynamic diameter) can be written as:

$$D_h = A \times W_0 \qquad (2)$$

Then, it is possible to determine (a) the value of parameter *A*, which is the slope of the D-W_0 line, in this case being of ca. 0.5, and (b) the W_0 value for the *residual micelles left after hydrate formation*, which, as shown in Figure 3, is of ca. 9 (intersection of the two linear fitting curves). In this way, it is possible to demonstrate that at least part of unconverted water remains trapped into reversed micelles while the formed hydrate is separated as a solid or slurry phase, which is easily separable and recoverable from the liquid system. In any event, gravimetric calculations were made by taking into account total added water. A summary list of DLS data for the other co-formers is reported below in Table 2.

Table 2 - Values of reverse micelle diameters vs. W_0 before and after hydrate formation

Co-former	W_0	D_1, nm[a]	D_2, nm[b]
THF	25	13	4.7
	50	24	4.7
	80	40	4.7
CP	25	10	4.4
	50	23	4.5
	80	35	4.4
DXL	25	10	4.8

	50	25	4.8
	80	41	4.5
DHF	25	11	4.9
	50	20	4.7
	80	36	4.7
THT	25	12	5.0
	50	22	4.9
	80	39	4.9
THP	25	10	4.4
	50	20	4.4
	80	37	4.5

[a] Diameter of water pool before hydrate formation; [b] Diameter after hydrate formation. All DLS measurements showed a coefficient of variation <20%, i.e. sizes are monodisperse. For a discussion, see section 2.3 above.

A *co-former* in a binary hydrate has the role to stabilize the (larger) hydrate cages, thus allowing hydrogen to remain entrapped into the smaller cages (even if a stabilizing role of hydrogen itself has also been proposed).[42,43] In hydrate-forming reverse micelles, the organic solvent may also have a dual function as both the dispersing medium *and* the clathrate *co-former*. This could help when the supply of co-former from the organic dispersing medium would not take place at a sufficient rate in cases where the co-former had such a partition coefficient as to remain essentially in the bulk organic phase. For those reasons, it is important to study the properties of several co-formers, other than the well-known THF. In the present work, we also tested cyclopentane (CP), dioxolane (DXL), dihydrofuran (DHF), tetrahydropyran (THP), and tetrahydrothiophene (THT). The supramolecular mechanisms through which an organic molecule can induce stabilization of clathrate cages are not clear. A hypothesis is that the presence of heavier molecules into the larger cages induces a distortion in the smaller ones, such a distortion inducing a change in the energy quantum levels of the hydrogen contained into the cage.[44]

By following the reverse micelle process described above, we formed binary clathrates of stoichiometric (i.e., ca. 5.56 mol%) co-formers (THF, CP, DXL, DHF, THP, and THT) with

hydrogen. Hydrogen uptake was determined under constant-pressure by measuring the quantity of H_2 flowing into the reactor after hydrate formation starts. In fact, when hydrates begin to form, hydrogen is increasingly captured within the hydrate crystals, and its pressure inside the reactor starts to decrease, calling for a restoration of the setpoint pressure by the PID controller. This event is clearly visible as a sudden increase in temperature within the bulk liquid (hydrate formation is exothermic), which is accompanied by a remarkable increase of gas absorption as read through the thermal mass flow meter (see section 2.2). Values of normalized gravimetric contents of hydrogen into hydrate can then be calculated according to the following equation:

$$\frac{H_2(g)}{H_2O(g)+H_2(g)} \times 100 \qquad (3),$$

where $H_2(g)$ is the mass (grams) of absorbed hydrogen, and $H_2O(g)$ is the mass of total water in the reverse micelle. Note that, as compared to the values reported in Table 3, the weight percent of hydrogen into hydrate will increase when using the effective mass of water taking part into hydrate formation, i.e., total water minus water bound to AOT head groups (see the above discussion on light scattering data).

Figure 4 reports the experimental traces of the integrated gas volume readings from the mass flow meter, and temperature profiles for the six co-formers studied. It is clearly seen that a massive hydrogen uptake starts as soon as hydrate formation begins and temperature starts to increase.

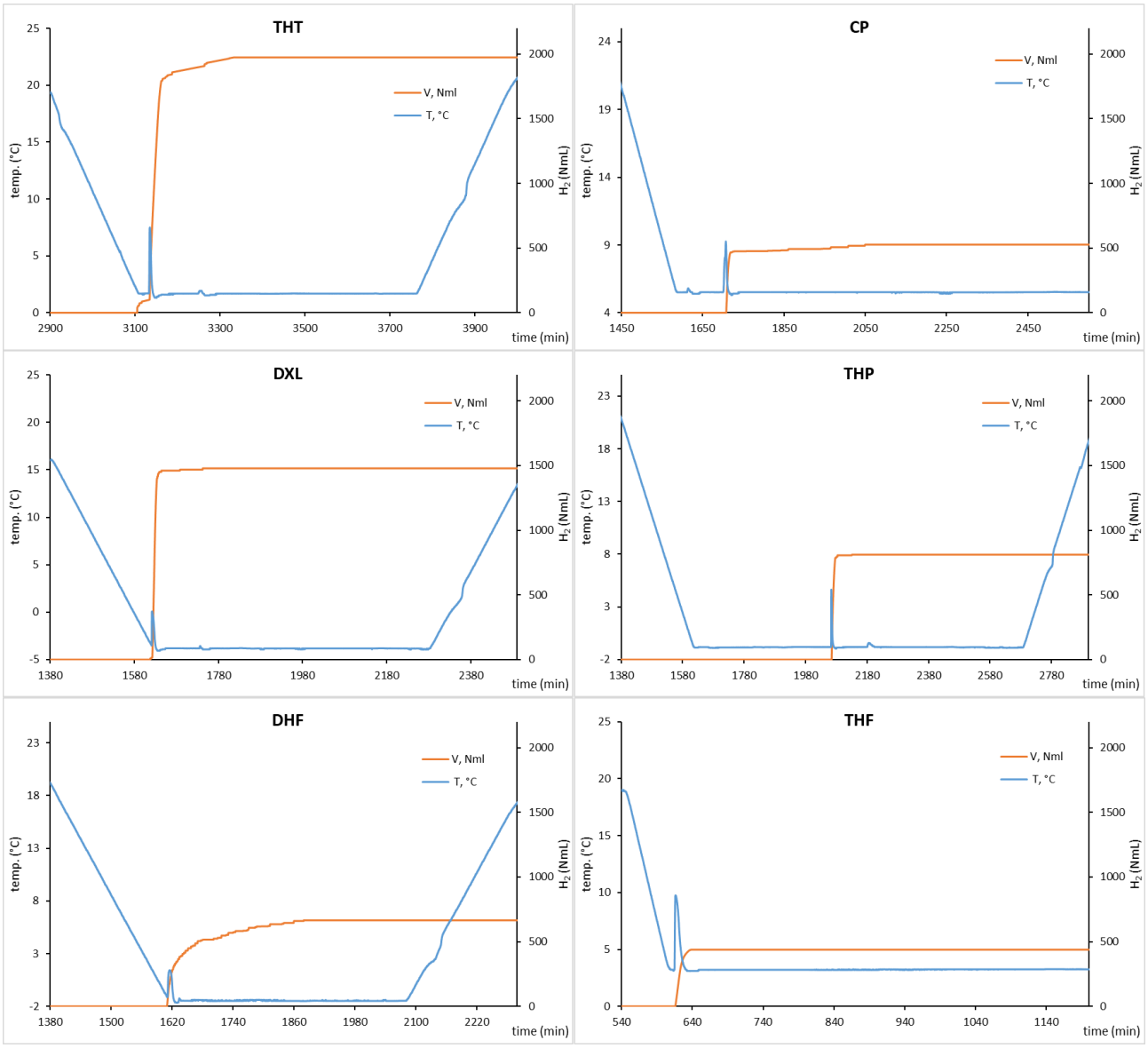

Figure 4. Experimental traces of integrated gas flow (Nml; orange) and temperature (°C; cyan) profiles for the six co-formers studied.

Table 3 below reports the relative amounts of stored hydrogen as calculated with eq. 3, and the kinetics of hydrate formation. Incidentally, it should be added that attempts to form binary hydrates of water-insoluble co-formers (e.g., CP, THT) with H_2 failed, within an experimentally reasonable time span of several hours, when using an usual setup formed by a biphasic system of co-former/water kept under H_2 pressure and vigorous stirring.

Table 3 - Summary of gravimetric H_2 contents and process kinetics for tested co-formers. Values in parentheses are coefficients of variations (%)

Co-former	%wt H_2 (±0.01)	Formation times, min[a]	Induction times, min[b]
CP	0.11	14 (8%)	11
DHF	0.16	190 (14%)	immediate[c]
DXL	0.36	18 (8%)	immediate[c]
THP	0.19	13 (9%)	24
THT	0.50	28 (10%)	3
THF	0.12	19 (5%)	immediate[c]

[a] Time from onset of exotherm to completion of absorption.
[b] Minutes elapsed before hydrate formation starts, after the system has reached target P, T. Reported values are the shortest times observed among triplicate experiments. It should be noted that, given the inherent stochasticity of induction times, triplicate experiments were not sufficient to get a reliable coefficient of variation.
[c] Hydrate forms as soon as T reaches target value.

There are several papers in the literature comparing the properties and phase equilibria of binary H_2 hydrates with various co-formers,[20,23,45] and differences in hydrate stabilization efficiencies are variously ascribed to properties such as molecular geometry, dipole moment, van der Waals radius etc. Generally, the gravimetric H_2 content values observed in the literature broadly agree with those found in the present work, with e.g. a 0.1 wt% reported for THF in a similar time span,[24] and a 0.6 wt% described for THT,[20] the latter also showing a faster kinetics as compared to THF. Solubility in, and/or partition between, water/organic solvent does not seem to be of any relevance as can be seen from the values of n-octanol/water partition coefficients of the two best performers in terms of H_2 uptake (logP(THT) = 1.4; logP(DXL) = -0.4; cf. Table 4). This finding is intriguing as it seems to point to the importance of the kinetics of the overall process: in other words, even when we have a very hydrophobic co-former (e.g., THT) the availability of a myriad water nano-interfaces will lead to plenty of co-former molecules in the proximity of those interfaces, which are readily uptaken when hydrate formation starts. On the other hand, regardless of the hydrophobicity of the co-former, it is observed that best performers are those molecules with a

remarkably larger polar surfaces, as quantified by the topological polar surface areas reported in Table 4. It is known that co-former establish weak (i.e., London), stabilizing interaction with hydrate cages,[46] then it comes with no surprise that a large, polarizable moiety (e.g., sulfur in THT) acts as a stronger inducer of hydrate formation, than, e.g., cyclopentane. Generally, the efficiency of hydrogen uptake broadly follows the order of topological polar surface areas reported in Table 4.

Table 4. Selected co-former properties[a]

Properties	**THF**	**THT**	**DXL**	**2,5-DHF**	**CP**	**THP**
MW	72.107 g/mol	88.168 g/mol	74.079 g/mol	70.091 g/mol	70.135 g/mol	86.134 g/mol
Topological polar surface area	9.2 $Å^2$	25.3 $Å^2$	18.5 $Å^2$	9.2 $Å^2$	0 $Å^2$	9.2 $Å^2$
LogP	0.5	1.4	-0.4	0.5	3	0.9

[a]Source: U.S. National Library of Medicine, NCBI (pubchem.ncbi.nlm.nih.gov)

4. Conclusions

With the aim of finding enhanced methods for hydrogen storage into hydrates, it is important to overcome the remarkable kinetic hindrance to hydrate formation, without adding further weight to the system and, desirably, while keeping a process which is simple and amenable to scale-up. The basic idea that we followed in the development of the process presented here was to increase the gas-water interfacial area by forming "nanodroplets" of water stabilized by a shell of surfactant molecules. Water droplets typically ranged from a few to tens of nanometers, according to the amount of added water. The present method for making binary hydrogen hydrates proved moderately effective in terms of gravimetric H_2 storage, as it gave up to about 0.5 wt% of H_2 entrapped with tetrahydrothiophene as a co-former, as calculated by integrating high-precision gas

flow data. According to the literature, this value corresponds to a usable energy content higher than that stored into 20 MPa-hydrogen of the same weight.[36] More importantly, the kinetics of the process was much faster as compared to known, top-down processes,[24-26] which require previous formation of a solid hydrate with a co-former, then pressurization with H_2. Methods such as those described by Strobel are moderately effective when the co-former is soluble/miscible in water (e.g., THF), but become more cumbersome when dealing with water-insoluble compounds, such as CP and THT. Hydrates formed within reverse micelles seem to be less dependent on the water solubility of the co-former, gas absorption being complete within time spans which are comparable among hydrophilic and hydrophobic compounds.

We believe that the obtained performance was due the huge increase of surface-to-volume ratio of water available to interact with hydrogen dissolved into the bulk organic phase, as compared to, e.g., a bulk aqueous phase, or 50-micron ice granules in contact with a hydrogen atmosphere. Furthermore, the enhanced solubility of hydrogen into hydrocarbons, e.g. iso-octane, as compared to that in water, may be playing a role in causing a faster transfer of H_2 within the hydrate-forming, aqueous *pseudo-phase*. Finally, the bulk medium may act as a "buffer" for controlling the water solubility of certain water-miscible co-formers, or enhancing the co-former/water contact for water-immiscible molecules. The role of the co-former in the stabilization of large cages in H_2 hydrates is crucial, therefore a deeper understanding of the molecular/supramolecular mechanisms underlying its effects should be gained. Further studies should also focus on the design and synthesis of novel molecules which are more effective as reverse micelle stabilizers.

Hydrogen storage technologies in compressed or liquefied form are still without competitors as compared to the "novel" technologies based on metal hydrides, carbon nanotubes, covalent hydrogenated compounds (ammonia), etc., even if enthusiasm with the established approaches is fading as the inherent difficulties and energetic costs thereof are clarified.[36] Although an

industrially feasible hydrogen storage technology based on clathrate hydrates seems out of reach at present, nevertheless attempts are already being made to exploit their potential.[47-49]

References

1. P. Preuster, A. Alekseev, P. Wasserscheid, Hydrogen Storage Technologies for Future Energy Systems, *Annu. Rev. Chem. Biomol. Eng.* 8 (2017) 445–471. doi:10.1146/annurev-chembioeng-060816-101334.
2. X. Yu, Z. Tang, D. Sun, L. Ouyang, M. Zhu, Recent advances and remaining challenges of nanostructured materials for hydrogen storage applications, *Prog. Mater. Sci.* 88 (2017) 1–48. doi:10.1016/j.pmatsci.2017.03.001.
3. H. Blanco, A. Faaij, A review at the role of storage in energy systems with a focus on Power to Gas and long-term storage, *Renew. Sustain. Energy Rev.* 81 (2018) 1049–1086. doi:10.1016/j.rser.2017.07.062.
4. L.E. Klebanoff, J.O. Keller, 5 Years of hydrogen storage research in the U.S. DOE Metal Hydride Center of Excellence (MHCoE), *Int. J. Hydrogen Energy.* 38 (2013) 4533–4576. doi:10.1016/j.ijhydene.2013.01.051.
5. R. Drnevich, Hydrogen Delivery, Liquefaction & Compression, Praxair – Tonawanda, NY (2003) 20.
6. N. Sirosh, A. Abele, A. Niedzwiecki; Section III. Hydrogen Storage- III. A High Pressure Tanks, Hydrogen, Fuel Cells, and Infrastructure Technologies. DOE – QUANTUM Tech - FY 2002 Progress Report.
7. A. T-Raissi, A. Banerjee, K. Sheinkopf, Metal Hydride Storage Requirements for Transportation Applications, *Florida Solar Energy Center* (1996) 2280–2285.

8. E. D. Sloan, C. A. Koh, Clathrate Hydrates of Natural Gases, 3rd ed.; CRC Press, Taylor & Francis Group: Boca Raton, FL, 2008.
9. N. Daraboina, J. Ripmeester, V.K. Walker, P. Englezos, Natural Gas Hydrate Formation and Decomposition in the Presence of Kinetic Inhibitors. 3. Structural and Compositional Changes, *Energy & Fuels.* 25 (2011) 4398–4404. doi:10.1021/ef200814z.
10. J. Carroll, Natural Gas Hydrates – A Guide for Engineers, Gulf Professional Publishing, Elsevier Science, MA, 2003.
11. P. Di Profio, V. Canale, N. D'Alessandro, R. Germani, A. Di Crescenzo, A. Fontana, Separation of CO_2 and CH_4 from biogas by formation of clathrate hydrates: Importance of the driving force and kinetic promoters, *ACS Sustain. Chem. Eng.* 5 (2017) 1990–1997. doi:10.1021/acssuschemeng.6b02832.
12. P. Di Profio, S. Arca, R. Germani, G. Savelli, Novel nanostructured media for gas storage and transport: Clathrate hydrates of methane and hydrogen, *J. Fuel Cell Sci. Technol.* 4 (2007) 49–55. doi:10.1115/1.2393304.
13. S. Arca, P. Di Profio, R. Germani, G. Savelli, European Patent Publication EP 2160352, 2010.
14. A. Di Crescenzo, P. Di Profio, G. Siani, R. Zappacosta, A. Fontana, Optimizing the Interactions of Surfactants with Graphitic Surfaces and Clathrate Hydrates, *Langmuir*. 32 (2016) 6559–6570. doi:10.1021/acs.langmuir.6b01435.
15. Y.A. Dyadin, E.G. Larionov, A.Y. Manakov, F.V. Zhurko, E.Y. Aladko, T.V. Mikina, V.Y. Komarov, Clathrate hydrates of hydrogen and neon, *Mendeleev Commun.* 9 (1999) 209–210. doi:10.1070/MC1999v009n05ABEH001104.
16. Y.A. Dyadin, É.G. Larionov, E.Y. Aladko, A.Y. Manakov, F.V. Zhurko, T.V. Mikina, V.Y. Komarov, E.V. Grachev, Clathrate formation in water-noble gas (Hydrogen) systems at high pressures, *J. Struct. Chem.* 40 (1999) 790–795. doi:10.1007/BF02903454.

17. W.L. Mao, Hydrogen Clusters in Clathrate Hydrate, *Science* 297 (2002) 2247–2249. doi:10.1126/science.1075394.
18. Mao et al. U.S. Pat. No. 6,735,960, "Composition and Method for Hydrogen Storage", issued May 18, 2004.
19. L.J. Florusse, C.J. Peters, J. Schoonman, K.C. Hester, C.A. Koh, S.F. Dec, K.N. Marsh, E.D. Sloan, Stable Low-Pressure Hydrogen Clusters Stored in a Binary Clathrate Hydrate, *Science* 306 (2004) 469–471. doi:10.1126/science.1102076.
20. H.P. Veluswamy, R. Kumar, P. Linga, Hydrogen storage in clathrate hydrates: Current state of the art and future directions, *Appl. Energy.* 122 (2014) 112–132. doi:10.1016/j.apenergy.2014.01.063.
21. J. Liu, J. Hou, J. Xu, H. Liu, G. Chen, J. Zhang, Ab initio study of the molecular hydrogen occupancy in pure H_2 and binary H_2 -THF clathrate hydrates, *Int. J. Hydrogen Energy.* 42 (2017) 17136–17143. doi:10.1016/j.ijhydene.2017.06.025.
22. S. Alavi, J.A. Ripmeester, Simulations of hydrogen gas in clathrate hydrates, *Mol. Simul.* 43 (2017) 808–820. doi:10.1080/08927022.2017.1295456.
23. A.T. Trueba, L.J. Rovetto, L.J. Florusse, M.C. Kroon, C.J. Peters, Phase equilibrium measurements of structure II clathrate hydrates of hydrogen with various promoters, *Fluid Phase Equilibria* 307, (2011) 6-10.
24. T.A. Strobel, C.J. Taylor, K.C. Hester, S.F. Dec, C.A. Koh, K.T. Miller, E.D. Sloan, Molecular hydrogen storage in binary THF-H_2 clathrate hydrates, *J. Phys. Chem. B.* 110 (2006) 17121–17125. doi:10.1021/jp062139n.
25. T.A. Strobel, K.C. Hester, C.A. Koh, A.K. Sum, E.D. Sloan, Properties of the clathrates of hydrogen and developments in their applicability for hydrogen storage, *Chem. Phys. Lett.* 478 (2009) 97–109. doi:10.1016/j.cplett.2009.07.030.

26. C.J. Peters, E.D. Sloan, Hydrogen Storage, US2007/179325.
27. K. Lokshin, Y. Zhao, Ice method for production of hydrogen clathrate hydrates, US 2006/0009664 A1.
28. G. Irvin, S. Li, B. Simmons, V. John, G. McPherson, M. Max, R. Pellenbarg, Control of Gas Hydrate Formation Using Surfactant Systems: Underlying Concepts and New Applications, *Ann. N. Y. Acad. Sci.* 912 (2000) 515–526. doi:10.1111/j.1749-6632.2000.tb06806.x.
29. E. Bayraktar, Ö. Kocapiçak, Ü. Mehmetoğlu, M. Parlaktuna, T. Mehmetoğlu, Recovery of amino acids from reverse micellar solution by gas hydrate, *Chem. Eng. Res. Des.* 86 (2008) 209–213. doi:10.1016/j.cherd.2007.12.001.
30. B. Liu, H. Liu, B. Wang, J. Wang, C. Sun, X. Zeng, G. Chen, Hydrogen separation via forming hydrate in W/O emulsion, *Fluid Phase Equilib.* 362 (2014) 252–257. doi:10.1016/j.fluid.2013.10.019.
31. S. Li, S. Fan, J. Wang, X. Lang, Y. Wang, Clathrate hydrate capture of CO_2 from simulated flue gas with cyclopentane/water emulsion, *Chinese J. Chem. Eng.* 18 (2010) 202–206. doi:10.1016/S1004-9541(08)60343-2.
32. A. Galfré, M. Kwaterski, P. Braîntuas, A. Cameirao, J.M. Herri, Clathrate hydrate equilibrium data for the gas mixture of carbon dioxide and nitrogen in the presence of an emulsion of cyclopentane in water, *J. Chem. Eng. Data.* 59 (2014) 592–602. doi:10.1021/je4002587.
33. M. Nakajima, R. Ohinura, Y.H. Mori, Clathrate hydrate formation from cyclopentane-in-water emulsions, *Ind. Eng. Chem. Res.* 47 (2008) 8933–8939. doi:10.1021/ie800949k.
34. P.J. Rensing, M.W. Liberatore, A.K. Sum, C.A. Koh, E. Dendy Sloan, Viscosity and yield stresses of ice slurries formed in water-in-oil emulsions, *J. Nonnewton. Fluid Mech.* 166 (2011) 859–866. doi:10.1016/j.jnnfm.2011.05.003.

35. H. Lee, J. Lee, D.Y. Kim, J. Park, Y.T. Seo, H. Zeng, I.L. Moudrakovski, C.I. Ratcliffe, J.A. Ripmeester, Tuning clathrate hydrates for hydrogen storage, *Nature.* 434 (2005) 743–746. doi:10.1038/nature03457.
36. P. Di Profio, S. Arca, F. Rossi, M. Filipponi, Comparison of hydrogen hydrates with existing hydrogen storage technologies: Energetic and economic evaluations, *Int. J. Hydrogen Energy.* 34 (2009) 9173–9180. doi:10.1016/j.ijhydene.2009.09.056.
37. D.E. Koppel, Analysis of Macromolecular Polydispersity in Intensity Correlation Spectroscopy: The Method of Cumulants, *J. Chem. Phys.* 57 (1972) 4814–4820. doi:10.1063/1.1678153.
38. S. Nave, J. Eastoe, R.K. Heenan, D. Steytler, I. Grillo, What is so special about Aerosol-OT? 2. Microemulsion systems, *Langmuir.* 16 (2000) 8741–8748. doi:10.1021/la000342i.
39. B.J. Berne and R. Pecora, "Dynamic Light Scattering", *Wiley, New York*, 1976.
40. S. Arca, P. Di Profio, R. Germani, G. Savelli, Apparatus for preparing and studying clathrate hydrates, WO/2007/122647.
41. P. Di Profio, R. Germani, G. Onori, A. Santucci, G. Savelli, C.A. Bunton, Relation between the Infrared Spectrum of Water and Decarboxylation Kinetics in Cetyltrimethylammonium Bromide in Dichloromethane, *Langmuir.* 14 (1998) 768–772. doi:10.1021/la970202h.
42. T.A. Strobel, C.A. Koh, E.D. Sloan, Water cavities of sH clathrate hydrate stabilized by molecular hydrogen, *J. Phys. Chem. B.* 112 (2008) 1885–1887. doi:10.1021/jp7110549.
43. A.R.C. Duarte, A. Shariati, L.J. Rovetto, C.J. Peters, Water Cavities of sH Clathrate Hydrate Stabilized by Molecular Hydrogen: Phase Equilibrium Measurements, *J. Phys. Chem. B.* 112 (2008) 1888–1889. doi:10.1021/jp7110605.

44. L. Ulivi, M. Celli, A. Giannasi, A.J. Ramirez-Cuesta, D.J. Bull, M. Zoppi, Quantum rattling of molecular hydrogen in clathrate hydrate nanocavities, *Phys. Rev. B - Condens. Matter Mater. Phys.* 76 (2007) 161401. doi:10.1103/PhysRevB.76.161401.
45. T. Kawamura, S. Takeya, M. Ohtake, T. Yamamoto, Enclathration of hydrogen by organic-compound clathrate hydrates. *Chem. Eng. Sci*. 66 (2011) 2417–2420 doi: 10.1016/j.ces.2011.03.002
46. J. Liu, J. Hou, J. Xu, H. Liu, G. Chen, J. Zhang, Ab initio study of the molecular hydrogen occupancy in pure H_2 and binary H_2-THF clathrate hydrates, *Int. J. Hydrogen Energy*, 42 (2017), 17136-17143. doi:org/10.1016/j.ijhydene.2017.06.025
47. P. Di Profio, S. Arca, R. Germani, G. Savelli, Prototype of fuel cell supplied with hydrogen hydrate, presented at the International Fair and Trade Exhibition "Energethica 2007", Fiera di Genova, 24-26 May, 2007.
48. K. Meier, Hydrogen production with sea water electrolysis using Norwegian offshore wind energy potentials, *Int. J. Energy Environ. Eng.* 5 (2014) 104. doi:10.1007/s40095-014-0104-6.
49. A. Possner, K. Caldeira, Geophysical potential for wind energy over the open oceans, *Proc. Natl. Acad. Sci.* (2017) 201705710. doi:10.1073/pnas.1705710114.

Graphical Abstract

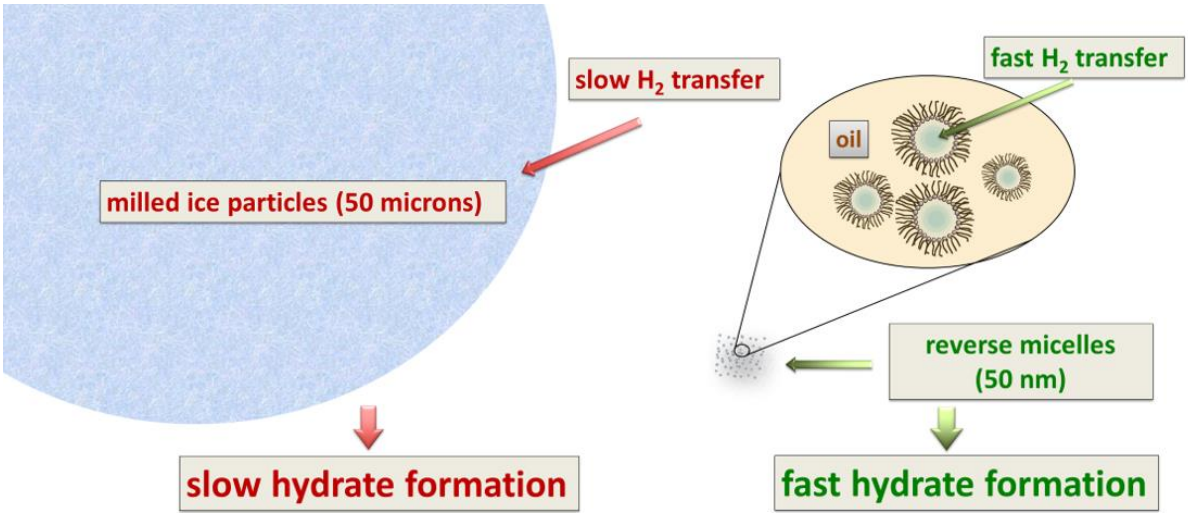

Highlights for manuscript:

REVERSE MICELLES ENHANCE THE FORMATION OF CLATHRATE HYDRATES OF HYDROGEN

(Authors: Pietro Di Profio,* Valentino Canale, Raimondo Germani, Simone Arca, Antonella Fontana)

- A reverse micelle process was used to enhance clathrate hydrates of hydrogen
- Hydrogen was stored into clathrate up to 0.5 wt% at 10 MPa
- Formation kinetics was in the order of minutes
- Water-insoluble co-guests were effectively used with the reverse micelle
- Enhancement of hydrate formation was due to a remarkable increase of surface-to-volume ratio of the water pseudo-phase.